

Dynamic origin-destination matrix estimation for networks operating under free-flow conditions using macroscopic flow dynamics

Yirolanda Englezou,^{*} Stelios Timotheou,^{*}
Christos G. Panayiotou^{*}

^{*} *KIOS Research and Innovation Center of Excellence, and the
Department of Electrical and Computer Engineering,
University of Cyprus*

{englezou.yirolanda, timotheou.stelios, christosp}@ucy.ac.cy

Abstract: The origin-destination (OD) matrix is a crucial requirement for efficient transportation planning, however its estimation still remains one of the most challenging tasks in transportation. This paper proposes a novel methodology for the estimation of dynamic OD matrices. The proposed methodology integrates disaggregated measurements from stationary sensors, e.g. loop detectors, with a macroscopic model that associates OD demands with traffic counts on specific network links. We investigate networks that operate under free-flow conditions, hence the dynamic OD matrix estimation problem is formulated as a linear mathematical program. Finally, we reformulate the problem to obtain a computationally cheap quadratic programming problem that allows real-time estimation of OD matrices within the time-window under study. We demonstrate the effectiveness of our methodology through a literature network, showcasing its ability to accurately capture travel patterns in a computationally efficient manner, allowing informed decision-making processes in transportation planning and management.

Keywords: demand estimation, dynamic origin-destination matrix estimation, cell transmission model, path demand, optimisation, traffic flow dynamics.

1. INTRODUCTION

The efficient estimation of the origin-destination (OD) matrix of a particular network of interest is a crucial requirement for the field of transportation that enables practitioners to better plan and manage the network, as well as researchers to validate novel monitoring and control methodologies. The OD matrix contains information on the number of vehicles that commute towards specific locations. In practice OD matrices cannot be directly observed, hence they have to be efficiently estimated using available information. Various methodologies have been proposed and validated over the years for the OD matrix estimation problem. There are two main OD matrix estimation problem variants considered, the *static* and the *dynamic* (or time-varying).

The static OD matrix estimation problem aims to find average time-independent OD demands over a fixed period of time. The common practice is to assume that a single set of link counts is available without taking into account time-dependent traffic flows (Chen et al., 2009; Hazelton, 2010). On the other hand the dynamic OD estimation problem is based on time-varying traffic counts in a sequence of intervals (for example every 10-15

minutes) and aims to estimate the corresponding time-varying OD matrices. The dynamic problem is designed for short-term traffic operation applications, such as route guidance, dynamic traffic assignment, traffic signal control and freeway corridor control (Ying et al., 2016; Marzano et al., 2018). Several methods have been proposed over the past decades to solve the static and dynamic OD matrix estimation problem; a good survey can be found in Bera and Rao (2011).

Most developed methodologies for the dynamic OD matrix estimation use the bi-level optimisation framework, assuming that a routing matrix is given and iterate between OD estimation and traffic assignment until some sort of convergence is achieved (Tavana and Mahmassani, 2001; Zhou et al., 2003). Bi-level programming in general is difficult to solve due to non-convexity and non-differentiability (Florian and Chen, 1995), hence it is a challenge to derive efficient algorithms for their solution (Zhang et al., 2017; Osorio, 2019). Many authors, e.g. Barceló et al. (2012), Cascetta et al. (2013), Marzano et al. (2018) among others, applied the Kalman-filtering technique for the dynamic OD matrix estimation problem. However, Kalman-filtering is optimal only when both the evolution and observation process are linear and subject to Gaussian noise, however these assumptions are often violated for several reasons, e.g. nonlinearity of flows in congested networks. Deep learning approaches that construct layered computational graphs have been developed more recently (Wu et al., 2018; Ma et al., 2020), however these approaches are computationally very demanding, hence not suitable for large-scale problems, while they yield locally optimal solutions due to the non-convexity of the problems (Wu et al., 2018). In

^{*} This work is supported by the European Union (i. ERC, URANUS, No. 101088124 and, ii. Horizon 2020 Teaming, KIOS CoE, No. 739551), and the Government of the Republic of Cyprus through the Deputy Ministry of Research, Innovation, and Digital Strategy. Views and opinions expressed are however those of the author(s) only and do not necessarily reflect those of the European Union or the European Research Council Executive Agency. Neither the European Union nor the granting authority can be held responsible for them.

most of these approaches a prior (or target) OD matrix, obtained from historic data is considered as input for the OD matrix estimation problem. A major drawback of this is that the OD estimation error may be large when the sample used to obtain the prior matrix is poor (Krishnakumari et al., 2020).

In contrast to the majority of the proposed methodologies for estimating dynamic OD matrices, which rely on prior (or target) matrices, or utilize extensive historical data, our approach leverages disaggregated measurements. These measurements involve breaking down traffic data into smaller intervals within a predefined time-window. Furthermore, to address shortcomings in existing models, we incorporate a macroscopic model that associates OD demands with traffic counts on specific network links. Flow propagation is captured with the use of the signalized path-based Cell Transmission Model (CTM) (Englezou et al., 2024). However, formulating the OD matrix estimation problem with disaggregated measurements and macroscopic traffic dynamics results in a complex, high-dimensional optimization problem. We address this challenge by developing an efficient solution methodology for free-flow scenarios. We validate the proposed approach on a standard literature network operating under free-flow conditions and conduct tests using full and partial measurements.

The remainder of the paper is organised as follows. In the next section (Section 2) we describe the structure of a basic traffic network and in Section 3 we formulate the dynamic OD matrix estimation problem. In Section 4 we give a brief introduction to the path-based CTM and the problem-specific dynamics. Section 5 focuses on the solution approach in the context of the path-based CTM. In Section 6 we present a simulation study to validate the proposed methodology. Section 7 outlines the main results of this work and suggests future research directions.

2. NETWORK NOTATION

Consider a traffic network with N nodes and W OD pairs, where $W \leq N \times (N - 1)$. The network is characterised by a fixed number of directed road links, each composed of multiple road segments, with \mathcal{L} the set of all road segments. We consider that there are fixed-location sensors that can estimate the density of a road segment, such that \mathcal{C} is the set of measured road segments with $\mathcal{C} \subseteq \mathcal{L}$, and \mathcal{W} is the set of OD pairs with $W = |\mathcal{W}|$. We denote as $L = |\mathcal{L}|$ the number of road segments and $C = |\mathcal{C}| \leq L$ the number of measured road segments that are equipped with static sensors, e.g. loop detectors.

The demand of each OD pair $w \in \mathcal{W}$ is carried by a set of candidate paths¹ \mathcal{S}_w , such that $\mathcal{P} = \cup_{w \in \mathcal{W}} \mathcal{S}_w$ is the set of all candidate paths. We assume that traffic traverses through a subset of these candidate paths, which implies that a number of candidate paths might carry zero demand. Each road segment $i \in \mathcal{L}$ is associated with at least one path $p \in \mathcal{P}_i$, where \mathcal{P}_i is the set of all candidate paths and $P_i = |\mathcal{P}_i|$ the total number of candidate paths that pass through road segment i , such that $\mathcal{P} = \cup_{i \in \mathcal{L}} \mathcal{P}_i$. The total number of paths for all road segments is given by $M = \sum_{i \in \mathcal{L}} P_i$ and the total number of paths in the network by $Q = |\mathcal{P}|$.

We consider the estimation of OD matrices over a time-horizon T . The estimation time-window duration consid-

ered is T^W , such that $N^W = T/T^W$ different OD matrices are derived over the entire time-horizon. The j -th estimation time-window is defined as $\mathcal{T}_j = \{\tau | \tau_{j-1} \leq \tau \leq \tau_j\}$, $j \in \mathcal{N}^W = \{1, \dots, N^W\}$, such that $\tau_{N^W} - \tau_0 = T$ and $\tau_j - \tau_{j-1} = T^W$, $\forall j \in \mathcal{N}^W$.

3. PROBLEM FORMULATION

We consider networks that operate under free-flow conditions for the total time-horizon under study T . We split the time-window of interest \mathcal{T}_j into K time-steps of duration T_s [hours], and define $\mathcal{T}_j^+ = \{1, \dots, K\}$ and $\mathcal{T}_j = \{0, \dots, K - 1\}$, such that $K = T^W/T_s$, $\forall j \in \mathcal{N}^W$. Time-step duration T_s is used to characterize both the periodicity of measurements and the discrete time-step of the chosen traffic model. We consider a mathematical description of the physical system, given the free-flow conditions, which consists of a traffic state evolution model and an observation model described by

$$\begin{aligned} \mathbf{x}_{k+1} &= \mathbf{A}_k \mathbf{x}_k + \mathbf{B}_k \mathbf{u}^{(j)} + \boldsymbol{\epsilon}_k, \\ \mathbf{y}_k &= \mathbf{H}_k \mathbf{x}_k + \boldsymbol{\omega}_k, \end{aligned} \quad (1)$$

$j \in \mathcal{N}^W$ and $k \in \mathcal{T}_j$. Above, $\mathbf{x}_k \in \mathbb{R}^{(L+M) \times 1}$ is the state vector, \mathbf{x}_0 denotes the initial conditions of the process in time-window \mathcal{T}_j , $\mathbf{u}^{(j)} \in \mathbb{R}^{Q \times 1}$ is the unknown input vector in time-window \mathcal{T}_j and $\mathbf{y}_k \in \mathbb{R}^{C \times 1}$ are conditionally independent noisy observations. We assume that the initial vector $\mathbf{x}_0 \sim N(\boldsymbol{\mu}_0, \mathbf{R}_0)$, where both the mean $\boldsymbol{\mu}_0$ and variance \mathbf{R}_0 of the distribution are known. The state \mathbf{x}_K in time-window \mathcal{T}_j is obtained after estimating the unknown input vector $\mathbf{u}^{(j)}$ and is utilised as the initial state of time-window \mathcal{T}_{j+1} , $\forall j \in \mathcal{N}^W$.

Matrices $\mathbf{A}_k \in \mathbb{R}^{(M+L) \times (M+L)}$ and $\mathbf{H}_k \in \mathbb{R}^{C \times (M+L)}$ are defined as the evolution matrix of the unknown states as time progresses and the matrix of explanatory variables, respectively. Matrix \mathbf{H}_k and $\mathbf{B}_k \in \mathbb{R}^{(M+L) \times Q}$ do not vary with time hence we drop subscript k and use \mathbf{H} and \mathbf{B} , respectively, for the remainder of this paper. We assume independent Gaussian errors for both equations, $\boldsymbol{\epsilon}_k \sim N(\mathbf{0}, \boldsymbol{\Sigma}_k^\epsilon)$ and $\boldsymbol{\omega}_k \sim N(\mathbf{0}, \mathbf{Z}_k^\omega)$. Matrices $\boldsymbol{\Sigma}_k^\epsilon \in \mathbb{R}^{(M+L) \times (M+L)}$ and $\mathbf{Z}_k^\omega \in \mathbb{R}^{C \times (M+L)}$ are the model and measurement error matrices, respectively.

The measurement vector \mathbf{y}_k denotes an observed traffic variable, e.g. the traffic density denoted by $\bar{\rho}(k)$, of the measured road segments of the network at time k , and \mathbf{x}_k the unobserved states denoted by $\boldsymbol{\rho}(k)$, e.g. the density of each candidate path on road segment i at time k , where $k \in \mathcal{T}_j$. We assume that the input vector $\mathbf{u}^{(j)} = [u_1^{(j)}, \dots, u_Q^{(j)}]^T$ represents traffic entering the network at each path $p = 1, \dots, Q$. Problem-specific dynamics are explicitly defined in Section 4.2.

Given Model (1) and the obtained measurements, we aim to select $\mathbf{u}^{(j)}$ in time-window \mathcal{T}_j , such that the states of the model are as close as possible to the measurements. This can be formulated as a convex constrained least squares problem of the form

$$\begin{aligned} \min_{\mathbf{x}_k, \mathbf{u}^{(j)}} \sum_{k \in \mathcal{T}_j} \frac{1}{2} \left\{ \|\mathbf{y}_{k+1} - \mathbf{H} \mathbf{x}_{k+1}\|_{[\mathbf{Z}_k^\omega]^{-1}}^2 \right. \\ \left. + \|\mathbf{x}_{k+1} - \mathbf{A}_k \mathbf{x}_k - \mathbf{B} \mathbf{u}^{(j)}\|_{[\boldsymbol{\Sigma}_k^\epsilon]^{-1}}^2 \right\} \\ + \frac{1}{2} \|\mathbf{x}_0 - \boldsymbol{\mu}_0\|_{[\mathbf{R}_0]^{-1}}^2 \end{aligned}$$

¹ Candidate paths can be generated using a variation of the k-shortest paths algorithm for transportation networks which identifies the top shortest paths that are significantly different in terms of the road segments used.

$$\mathbf{x}_k \geq \mathbf{0}, \quad k \in \mathcal{T}_j, \quad \mathbf{u}^{(j)} \geq \mathbf{0}, \quad (2)$$

where \mathbf{x}_k and $\mathbf{u}^{(j)}$ are the optimisation variables. The proposed problem (2) for dynamic path-based OD matrix estimation can be challenging due to the high dimensionality of vectors \mathbf{x}_k that have to be estimated at each time-step $k \in \mathcal{T}_j$.

By obtaining $\mathbf{u}^{(j)}$ through the solution of Problem (2), the demand of each OD pair in time-window $\mathcal{T}_j, \forall j \in \mathcal{N}^W$, can be simply obtained by

$$\sum_{p \in \mathcal{S}_w} u_p^{(j)} = d_w^{(j)}, \quad \forall w \in \mathcal{W}, \quad \forall j \in \mathcal{N}^W. \quad (3)$$

4. MACROSCOPIC FLOW MODEL

The cell transmission model (CTM) is a macroscopic flow model (Daganzo, 1995) and is widely used in traffic applications (control, modelling, study stabilisation of road networks). Each cell i is characterised by: the maximum speed in free flow, v_i^f (km/h), the backward propagation speed v_i^b (km/h), the maximum flow, φ_i^{max} (veh/h), the maximum density, ρ_i^{max} (veh/km) and the length l_i of the cell. Note that a vehicle cannot enter and exit from cell i within one time-step, hence the model must satisfy the Courant-Friedrichs-Lewy condition for stability (Grandinetti et al., 2018). Following Englezou et al. (2024), the inflow, $\varphi_i^{in}(t)$, and outflow, $\varphi_i^{out}(t)$, of vehicles of each cell i are defined by the boundary connections between consecutive cells. The upstream connection of each cell, i^- , may be categorised as ordinary, \mathcal{O} , entering, \mathcal{E} , or merging, \mathcal{M} , while the downstream connection, i^+ , can be ordinary, \mathcal{O} , diverging, \mathcal{D} , or exiting, \mathcal{G} .

4.1 Path-based cell transmission model

The path-based CTM (Ukkusuri et al., 2012) extends the capabilities of the traditional CTM by keeping track of path-based densities and flows, without necessitating strong assumptions on split ratios. Employing the path-based CTM enables the efficient estimation of the OD matrix by deriving path demands and utilizing Equation (3). The density corresponding to each path p traversing cell i is expressed as follows:

$$\rho_{i,p}(k+1) = \rho_{i,p}(k) + \frac{T_s}{l_i} [\varphi_{i,p}^{in}(k) - h_i(k)\varphi_{i,p}^{out}(k)]. \quad (4)$$

Above, $h_i(k)$ represents the traffic signal regulating the outbound traffic of cell $i \in \mathcal{L}$ through an alternating sequence of green ($h_i(k) = 1$) and red ($h_i(k) = 0$) phases. In networks operating under free-flow conditions and for $i^- \in \mathcal{O}, \mathcal{M}$, the inflow is determined by $\varphi_{i,p}^{in}(k) = v_j^f \rho_{j,p}(k)$, for $p \in \mathcal{P}_i \cap \mathcal{P}_j$ and j belonging in the set of upstream neighbours of i , i.e. $\in \mathcal{N}_i^-$, while for $i^- \in \mathcal{E}$, the inflow is given by $\varphi_{i,p}^{in}(k) = u_p$. Here, u_p exists only for entry connections and denotes vehicles entering the network at each time-step k . Similarly, for networks operating under free-flow conditions and for $i^+ \in \mathcal{O}, \mathcal{D}, \mathcal{G}$, the outflow is determined by $\varphi_{i,p}^{out}(k) = v_i^f \rho_{i,p}(k)$, for $p \in \mathcal{P}_i \cap \mathcal{P}_j$ and j in the set of downstream neighbours of i , i.e. $\in \mathcal{N}_i^+$. Here, the sets \mathcal{P}_i and \mathcal{P}_j denote all paths passing through cells i and j , respectively. It is important to note that the relationship between the path-based CTM and the standard CTM lies in the fact that the density, inflow, and outflow of cell i are expressed as the summation of per

path densities, inflows, and outflows associated with that particular cell, respectively:

$$\bar{\rho}_i(k) = \sum_{p \in \mathcal{P}_i} \rho_{i,p}(k)$$

$$\bar{\varphi}_i^{in}(k) = \sum_{p \in \mathcal{P}_i} \varphi_{i,p}^{in}(k), \quad \bar{\varphi}_i^{out}(k) = \sum_{p \in \mathcal{P}_i} \varphi_{i,p}^{out}(k).$$

For more details, see Englezou et al. (2024).

4.2 Problem-specific Dynamics

For the definition of Model (1) under the path-based CTM we have the $(M+L)$ -state vector given by $\mathbf{x}_k = \boldsymbol{\rho}(k)$. The Q average input vector $\mathbf{u}^{(j)}$, denotes the inflow of cell i at each time-step $k \in \mathcal{T}_j$, with $i^- \in \mathcal{E}$ and $p \in \mathcal{P}_i$. The set of observations, denoted by the C -vector $\mathbf{y}_k = [\bar{\rho}b_1(k), \dots, \bar{\rho}b_C(k)]^T \in \mathbb{R}^{C \times 1}$, obtained from loop detectors, where $C \leq L$, and $b_1, \dots, b_C \in \mathcal{C}$, comprises measurements taken on a subset (or all) of cells at time $k \in \mathcal{T}_j^+$. These observations are linked to the state vector via the matrix $\mathbf{H} \in \mathbb{R}^{C \times M}$.

5. SOLUTION APPROACH

In this section we describe a solution approach for Problem (2) utilising the path-based CTM, for networks that operate under free-flow conditions $\forall k \in \mathcal{T}_j$.

As described in Section 3, we consider Model (1) to describe the evolution of traffic density of the path-based CTM, that yields the convex constrained least squares problem (2). We will refer to this problem as the dynamic OD matrix least squares estimation, DOD_{LS}. Through this formulation, we aim to obtain vectors \mathbf{x}_k and $\mathbf{u}^{(j)}$ while minimising the estimation error in the objective function. The above formulation is computational heavy due to the high dimensionality of vectors \mathbf{x}_k that have to be estimated at each time-step $k \in \mathcal{T}_j^+$, preventing the estimation of the OD matrix of interest in real-time. In order to reduce the high dimensionality of \mathbf{x}_k , we reformulate the problem to obtain a lower-dimensional quadratic program.

5.1 Real-time Dynamic OD matrix estimation

To facilitate the real-time solution of the problem through a computationally efficient manner, we reformulate the dynamic OD matrix estimation problem as follows.

Expanding the state evolution model in (1) yields

$$\mathbf{x}_1 = \mathbf{A}_0 \mathbf{x}_0 + \mathbf{B} \mathbf{u}^{(j)} + \boldsymbol{\epsilon}_0,$$

$$\mathbf{x}_2 = \mathbf{A}_1 \mathbf{A}_0 \mathbf{x}_0 + \mathbf{A}_1 \mathbf{B} \mathbf{u}^{(j)} + \mathbf{A}_1 \boldsymbol{\epsilon}_0 + \mathbf{B} \mathbf{u}^{(j)} + \boldsymbol{\epsilon}_1.$$

We set $\mathbf{D}_2 = \mathbf{A}_1 \mathbf{A}_0$, $\mathbf{E}_2 = (\mathbf{A}_1 + \mathbf{I})$ and $\boldsymbol{\Delta}_2 = \mathbf{A}_1 \boldsymbol{\epsilon}_0 + \boldsymbol{\epsilon}_1$, hence $\mathbf{x}_2 = \mathbf{D}_2 \mathbf{x}_0 + \mathbf{E}_2 \mathbf{B} \mathbf{u}^{(j)} + \boldsymbol{\Delta}_2$. Following, we have that $\mathbf{x}_3 = \mathbf{A}_2 \mathbf{D}_2 \mathbf{x}_0 + (\mathbf{A}_2 \mathbf{E}_2 + \mathbf{I}) \mathbf{B} \mathbf{u}^{(j)} + \mathbf{A}_2 \mathbf{A}_1 \boldsymbol{\epsilon}_0 + \mathbf{A}_2 \boldsymbol{\epsilon}_1 + \boldsymbol{\epsilon}_2$, and we set $\mathbf{D}_3 = \mathbf{A}_2 \mathbf{D}_2$, $\mathbf{E}_3 = (\mathbf{A}_2 \mathbf{E}_2 + \mathbf{I})$ and $\boldsymbol{\Delta}_3 = \mathbf{A}_2 \boldsymbol{\Delta}_2 + \boldsymbol{\epsilon}_2$. In a similar fashion, we can express the state \mathbf{x}_k with respect to the initial conditions \mathbf{x}_0 , for which we know that $\mathbf{x}_0 \sim N(\boldsymbol{\mu}_0, \mathbf{R}_0)$, and the unknown path demand $\mathbf{u}^{(j)}$ as $\mathbf{x}_{k+1} = \mathbf{D}_k \mathbf{x}_0 + \mathbf{E}_k \mathbf{B} \mathbf{u}^{(j)} + \boldsymbol{\Delta}_k$, where $\mathbf{D}_k = \mathbf{A}_{k-1} \mathbf{D}_{k-1}$ with $\mathbf{D}_1 = \mathbf{A}_0$, $\mathbf{E}_k = (\mathbf{A}_{k-1} \mathbf{E}_{k-1} + \mathbf{I})$ with $\mathbf{E}_1 = \mathbf{I}$ and $\boldsymbol{\Delta}_k = \mathbf{A}_{k-1} \boldsymbol{\Delta}_{k-1} + \boldsymbol{\epsilon}_{k-1}$ with $\boldsymbol{\Delta}_1 = \boldsymbol{\epsilon}_0$. Following from the model definition, $\boldsymbol{\Delta}_k$ follows a normal distribution such as $\boldsymbol{\Delta}_k \sim N(\mathbf{0}, \boldsymbol{\Lambda}_k)$, where

$$\boldsymbol{\Lambda}_k = \mathbf{A}_{k-1} \boldsymbol{\Lambda}_{k-1} \mathbf{A}_{k-1}^T + \boldsymbol{\Sigma}_{k-1}^\epsilon, \quad (5)$$

with $\boldsymbol{\Lambda}_1 = \boldsymbol{\Sigma}_0^\epsilon$.

We set $\mathbf{z}_k = \mathbf{D}_k \mathbf{x}_0 + \mathbf{\Delta}_k$ and the state equation becomes $\mathbf{x}_{k+1} = \mathbf{E}_k \mathbf{B} \mathbf{u}^{(j)} + \mathbf{z}_k$, which remains linear over time. Through the definition of \mathbf{z}_k , we have that it follows a normal distribution such as $\mathbf{z}_k \sim N(\boldsymbol{\mu}_k^z, \boldsymbol{\Sigma}_k^z)$, where

$$\begin{aligned} \boldsymbol{\mu}_k^z &= \mathbf{A}_{k-1} \boldsymbol{\mu}_{k-1}^z \\ \boldsymbol{\Sigma}_k^z &= \mathbf{\Lambda}_{k-1} + \mathbf{A}_{k-1} \mathbf{D}_{k-1} \mathbf{R}_0 \mathbf{D}_{k-1}^T \mathbf{A}_{k-1}^T \end{aligned} \quad (6)$$

with $\boldsymbol{\mu}_1^z = \mathbf{A}_0 \boldsymbol{\mu}_0$ and $\boldsymbol{\Sigma}_1^z = \mathbf{A}_0 \mathbf{R}_0 \mathbf{A}_0^T + \boldsymbol{\Sigma}_0^\epsilon$. Using the above result we re-write the observation model as $\mathbf{y}_{k+1} = \mathbf{H} \mathbf{E}_{k+1} \mathbf{B} \mathbf{u}^{(j)} + \mathbf{H} \mathbf{z}_{k+1} + \mathbf{w}_{k+1}$. Setting $\mathbf{c}_{k+1} = \mathbf{H} \mathbf{z}_{k+1} + \mathbf{w}_{k+1}$, which is the sum of two random Gaussian variables, we obtain a simpler form of the observation model $\mathbf{y}_{k+1} = \mathbf{H} \mathbf{E}_{k+1} \mathbf{B} \mathbf{u}^{(j)} + \mathbf{c}_{k+1}$, and $\mathbf{c}_k \sim N(\boldsymbol{\mu}_k^c, \boldsymbol{\Xi}_k^c)$. The mean $\boldsymbol{\mu}_k^c$ and variance $\boldsymbol{\Xi}_k^c$ are given by

$$\boldsymbol{\mu}_k^c = \mathbf{H} \mathbf{A}_{k-1} \boldsymbol{\mu}_{k-1}^z, \quad (7)$$

$$\boldsymbol{\Xi}_k^c = \mathbf{H} \mathbf{\Lambda}_{k-1} \mathbf{H}^T + \mathbf{H} \mathbf{A}_{k-1} \mathbf{D}_{k-1} \mathbf{R}_0 \mathbf{D}_{k-1}^T \mathbf{A}_{k-1}^T \mathbf{H}^T + \mathbf{Z}_k^w,$$

where $\mathbf{\Lambda}_{k-1}$ is defined through (5) and $\boldsymbol{\mu}_{k-1}^z$ through (6).

Hence, formulation (2) under free-flow conditions becomes a convex non-negative least squares problem of the form

$$\begin{aligned} \min_{\mathbf{u}^{(j)}} \sum_{k \in \mathcal{T}_j} \|\mathbf{y}_{k+1} - \mathbf{H} \mathbf{E}_{k+1} \mathbf{B} \mathbf{u}^{(j)} - \boldsymbol{\mu}_{k+1}^c\|_{[\boldsymbol{\Xi}_k^c]^{-1}}^2 \\ \mathbf{u}^{(j)} \geq \mathbf{0}, \end{aligned}$$

and setting $\boldsymbol{\zeta}_{k+1} = \mathbf{y}_{k+1} - \boldsymbol{\mu}_{k+1}^c$ yields

$$\begin{aligned} \min_{\mathbf{u}^{(j)}} \sum_{k \in \mathcal{T}_j} \|\boldsymbol{\zeta}_{k+1} - \mathbf{H} \mathbf{E}_{k+1} \mathbf{B} \mathbf{u}^{(j)}\|_{[\boldsymbol{\Xi}_k^c]^{-1}}^2 \\ \mathbf{u}^{(j)} \geq \mathbf{0}, \end{aligned} \quad (8)$$

which is equivalent to the Quadratic Programming (QP) problem

$$\begin{aligned} \min_{\mathbf{u}^{(j)}} \mathbf{u}^{(j)T} \mathbf{Q} \mathbf{u}^{(j)} + \mathbf{q}^T \mathbf{u}^{(j)} \\ \mathbf{u}^{(j)} \geq \mathbf{0}, \end{aligned} \quad (9)$$

where $\mathbf{Q} = \sum_{k \in \mathcal{T}_j} \mathbf{B}^T \mathbf{E}_k^T \mathbf{H}^T [\boldsymbol{\Xi}_k^c]^{-1} \mathbf{H} \mathbf{E}_k \mathbf{B} \in \mathbb{R}^{Q \times Q}$ and $\mathbf{q} = -2 \sum_{k \in \mathcal{T}_j} \mathbf{B}^T \mathbf{E}_k^T \mathbf{H}^T [\boldsymbol{\Xi}_k^c]^{-1} \boldsymbol{\zeta}_{k+1} \in \mathbb{R}^{Q \times 1}$. This problem is convex, as \mathbf{Q} is positive semidefinite and the non-negativity constraints form a convex feasible set. Problem (9) can be optimally solved in a fast and reliable manner using standard mathematical solvers.

We will refer to this problem as the dynamic OD matrix quadratic program estimation, DOD_{QP}.

6. SIMULATION RESULTS

The proposed dynamic OD matrix estimation framework is applied to the Nguyen-Dupuis network (Nguyen and Dupuis, 1984) that was extensively used as a case study in many works (see for example Ukkusuri et al. (2012)), shown in Figure 1. This network consists of 65 cells, 20 OD pairs and 70 pre-specified paths. The following CTM parameters are considered: $v_i^f = 60$ km/h, $v_i^b = 20$ km/h, $\varphi_i^{max} = 1500$ veh/h, $\rho_i^{max} = 100$ veh/km, $\rho_i^c = 25$ veh/km, $l_i \in [0.3, 0.8]$ km. The time-horizon under study is $T = 12$ hours and we estimate OD matrices in continuous time-windows of duration $T^W = 15$ minutes. In addition, we assume that the sampling time-step is $T_s = 10$ seconds and hence we observe measurements for $K = 90$ intervals per time-window \mathcal{T}_j , $\forall j \in \mathcal{N}^W$. Finally, both the measurements and the model are subject to Gaussian noise with zero mean and variance matrix $\mathbf{Z}_k^w = \sigma_\omega^2 \mathbf{I}$ and $\boldsymbol{\Sigma}_k^\epsilon = \sigma_\epsilon^2 \mathbf{I}$, $\forall k \in \mathcal{T}_j$, respectively, with $\sigma_\epsilon^2 = 3$ and $\sigma_\omega^2 = 2$.

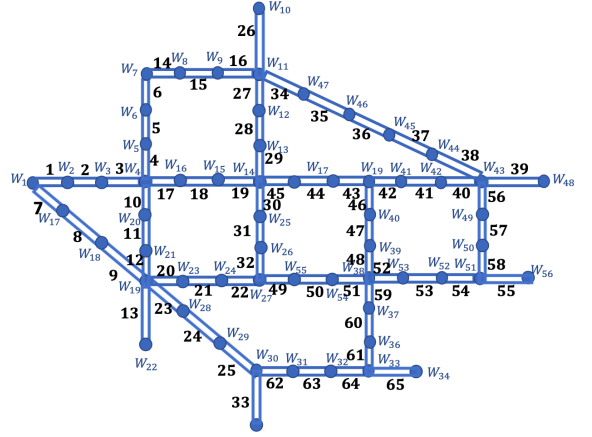


Fig. 1. Nguyen-Dupuis network.

Coverage	DOD _{LP}		DOD _{QP}	
	RMSE [veh/h]	MAPE [%]	RMSE [veh/h]	MAPE [%]
100%	2.17	5.3	2.09	4.9
80%	4.87	11.7	4.96	12.1
60%	11.97	16.6	12.12	17.3
40%	22.93	25.7	22.38	24.9

Table 1. Average RMSE and MAPE for different network coverage configurations using the DOD_{LP} and DOD_{QP} approaches.

Two loop detector configurations are examined:

- *Full coverage* of cells in the network under study and $C = L$ (100% coverage of the total number of cells).
- *Random partial coverage* of the cells in the network under study and $C < L$. We remove the loop detectors randomly from specific cells to obtain three scenarios: 80%, 60%, 40% coverage of the total number of cells.

We employ the framework for dynamic OD matrix estimation (Section 5), and compare estimation results using DOD_{LP} and the reformulated problem DOD_{QP}. The metrics used to compare the OD estimation performance of each algorithm are the root mean squared error (RMSE) and mean absolute percentage error (MAPE), given by

$$\text{RMSE} = \sqrt{\frac{1}{W} \sum_{w=1}^W (d_w^{(j)\text{true}} - d_w^{(j)})^2}, \quad (10a)$$

$$\text{MAPE} = \frac{1}{W} \sum_{w=1}^W \frac{|d_w^{(j)\text{true}} - d_w^{(j)}|}{d_w^{(j)\text{true}}} 100\%, \quad (10b)$$

where W is the total number of OD pairs, $d_w^{(j)\text{true}}$ is the true OD demand considered during the simulation for time-window \mathcal{T}_j and $d_w^{(j)}$ is the estimated OD demand in the same time-window \mathcal{T}_j .

First, we investigate the performance of the proposed methodology with respect to the accuracy of estimating the OD demand, assuming full or random partial coverage of the network. We run both optimisation procedures 50 times, while in each run we select a different subset of cells to ignore their measurements (in the case of random partial coverage), to mitigate potential biases in the results. In Table 1 we present average values across all time-windows under study, for both RMSE and MAPE

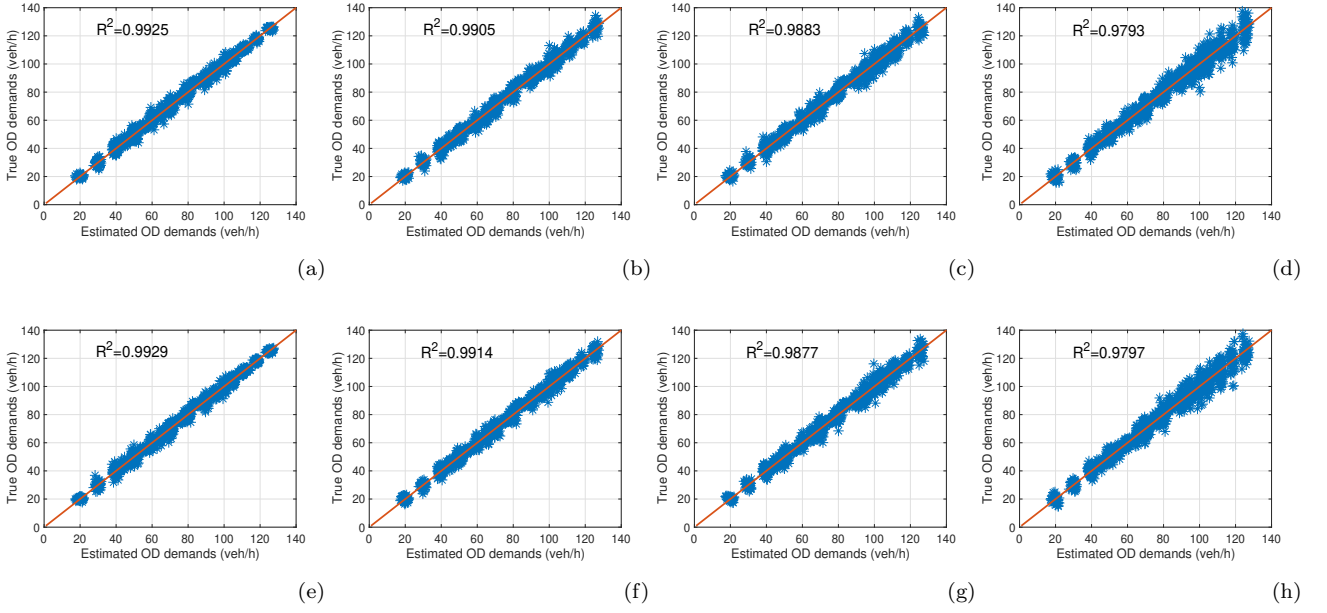


Fig. 2. Estimated, $\mathbf{d}^{(j)}$, against true, $\mathbf{d}^{(j)\text{true}}$, OD demands $\forall j \in \mathcal{N}^W$, and R^2 of the OD demands for the DOD_{LP} approach and (a) 100%, (b) 80%, (c) 60% (d) 40% network coverage and the DOD_{QP} approach and (e) 100%, (f) 80%, (g) 60% (h) 40% network coverage.

obtained through the application of DOD_{LP} and DOD_{QP} under different network coverage configurations.

The results presented in Table 1 indicate that reducing the network coverage percentage leads to higher values of both RMSE and MAPE for both solution methods. It is evident that both approaches yield similar results. The values of both metrics for the DOD_{LP} and the DOD_{QP} approach remain small, indicating accurate performance for both methodologies. Nevertheless, it is important to also assess the computational efficiency of the two approaches.

To further showcase the estimation performance of DOD_{LP} and DOD_{QP} for different percentages of network coverage, we present the estimated OD demands against the true OD demands, shown in Figure 2 and calculate the R^2 given by $R^2 = 1 - (d_w^{(j)\text{true}} - d_w^{(j)}) / (d_w^{(j)\text{true}} - \bar{d}^{(j)})$. The top row of plots corresponds to the DOD_{LP} approach, while the bottom row corresponds to the DOD_{QP} approach. Each plot in both rows represents estimation results obtained using varying percentages of network coverage, ranging from 100% to 40% (from left to right). As the cell coverage decreases for both approaches, the plots suggest slightly poorer estimates of the OD demands and increased fluctuation around the true OD demands. When comparing the DOD_{LP} approach (Figures 2 (a)-(d)) with the DOD_{QP} approach (Figures 2 (e)-(h)), the estimation results indicate a similar performance for both approaches across different network coverages.

Next, we analyse the average computational times of the proposed solution approaches, as presented in Table 2. As shown, the computational times demonstrate a consistent trend across different percentages of measurements. Notably, the DOD_{LP} approach appears more sensitive to the percentage of measurements compared to the DOD_{QP} approach, which exhibits robustness with respect to network coverage. However, it is crucial to highlight that the reformulated proposed solution, DOD_{QP} , achieves estimation results up to 60 times faster than the DOD_{LP} approach. This notable improvement in computational

Coverage	DOD_{LP} [s]	DOD_{QP} [s]
100%	3.7	0.068
80%	4.0	0.071
60%	4.8	0.078
40%	5.7	0.089

Table 2. Computational times (in seconds) under different percentages of network coverage.

efficiency shows great potential, especially for real-time dynamic estimation of OD matrices.

Finally, we choose two OD pairs (W_1W_{56} and $W_{10}W_{54}$) of the network to show the ‘real’ OD demand assumed during the simulation for all time-windows in the total horizon under study, as well as the estimated OD demands using the DOD_{LP} and DOD_{QP} approaches. For the results shown in Figure 3 we assume 80% (first column of plots) and 60% (second column of plots) of network coverage, while the first row of plots correspond to OD pair W_1W_{56} , while the second row corresponds to OD pair $W_{10}W_{54}$. The black line corresponds to the ‘true’ OD demand, the purple line to the DOD_{LP} approach, and the blue line to the DOD_{QP} approach. As shown, estimation results from both approaches are very similar and can closely replicate the ‘true’ OD demand and capture fluctuations across different time-windows. However, as the percentage of measurements decreases, the estimated OD demand begins to diverge more from the ‘true’ values.

7. CONCLUSIONS AND FUTURE WORK

This paper has investigated the dynamic OD matrix estimation problem. The proposed approach leverages disaggregated measurements and a macroscopic model that associates OD demands with traffic counts on specific network links, in contrast to the majority of the proposed methodologies for estimating dynamic OD matrices, that rely on prior (or target) matrices, or an extensive amount of historical data. Under these conditions, the resulting dynamic OD matrix estimation problem is a high-dimensional computational expensive optimization

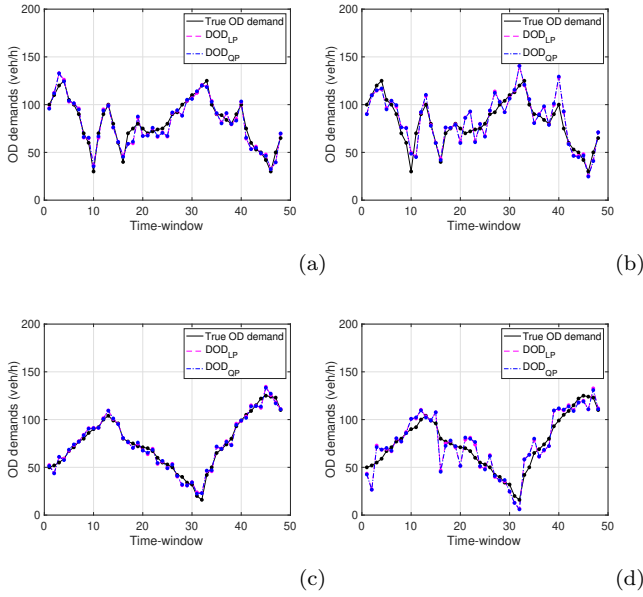


Fig. 3. OD demand for (a) W_1W_{56} OD pair and 80% of network coverage, (b) W_1W_{56} OD pair and 60% of network coverage, (c) $W_{10}W_{54}$ and 80% of network coverage, and (d) $W_{10}W_{54}$ and 60% of network coverage, for the total time-horizon T under study, across all different time-windows.

problem, especially for large networks. We address this challenge by reformulating the problem into a convex Quadratic Program, which can be optimally solved using standard optimisation tools. Results showed that the reformulated problem yields almost identical results with the initial formulation, while it can obtain an OD matrix in under 0.1 seconds, showcasing great potential, especially for real-time estimation of OD matrices.

Future work includes the extension of the proposed methodology to incorporate networks under congestion. In addition, we aim to investigate the efficiency of this approach in larger real-life networks.

REFERENCES

- Barceló, J., Montero, L., Bullesjos, M., Serch, O., and Carmona, C. (2012). A Kalman filter approach for the estimation of time dependent od matrices exploiting bluetooth traffic data collection. In *91st Transportation Research Board Annual Meeting*, 1–16. National Research Council, Washington, DC.
- Bera, S. and Rao, K.V.K. (2011). Estimation of origin-destination matrix from traffic counts: the state of the art. *European Transport*, 49, 3–23.
- Cascetta, E., Papola, A., Marzano, V., Simonelli, F., and Vitiello, I. (2013). Quasi-dynamic estimation of OD flows from traffic counts: formulation, statistical validation and performance analysis on real data. *Transportation Research Part B: Methodological*, 55, 171–187.
- Chen, A., Chootinan, P., and Recker, W. (2009). Norm approximation method for handling traffic count inconsistencies in path flow estimator. *Transportation Research Part B*, 43, 852–872.
- Daganzo, C.F. (1995). The cell transmission model, part II: network traffic. *Transportation Research B*, 79–93.
- Englezou, Y., Timotheou, S., and Panayiotou, C.G. (2024). Path-based origin-destination matrix estimation utilizing macroscopic traffic dynamics. *IEEE Transactions of Intelligent Transportation Systems*, 10.1109/TITS.2024.3370473.
- Florian, M. and Chen, Y. (1995). A coordinate descent method for the bi-level O-D matrix adjustment problem. *International Transactions in Operational Research* 2, 2, 165–179.
- Grandineti, P., Canudas-de Wit, C., and Garin, F. (2018). Distributed optimal traffic lights design for large-scale urban networks. *IEEE Transactions on Control System Technology*, 1–14.
- Hazelton, M.L. (2010). Bayesian inference for network-based models with a linear inverse structure. *Transportation Research Part B*, 44, 674–685.
- Krishnakumari, P., Van Lint, H., Djukic, T., and Cats, O. (2020). A data driven method for OD matrix estimation. *Transportation Research Part C*, 113, 38–56.
- Ma, W., Pi, X., and Qian, S. (2020). Estimating multi-class dynamic origin-destination demand through a forward-backward algorithm on computational graphs. *Transportation Research Part C: Emerging Technologies*, 119, 102747.
- Marzano, V., Papola, A., Simonelli, F., and Papageorgiou, M. (2018). A Kalman Filter for quasi-dynamic OD flow estimation/updating. *IEEE Transactions of Intelligent Transportation Systems*, 1–9.
- Nguyen, S. and Dupuis, C. (1984). An efficient method for computing traffic equilibria in networks with asymmetric transportation costs. *Transportation Science*, 18, 185–202.
- Osorio, C. (2019). Dynamic origin-destination matrix calibration for large-scale network simulators. *Transportation Research Part C: Emerging Technologies*, 98, 186–206.
- Tavana, H. and Mahmassani, H.S. (2001). Estimation of dynamic origin-destination flows from sensor data using bi-level optimization method. In *80th Transportation Research Board Annual Meeting*. Washington, DC.
- Ukkusuri, S.V., Han, L., and Doan, K. (2012). Dynamic user equilibrium with a path based cell transmission model for general traffic networks. *Transportation Research Part B*, 46, 1657–1684.
- Wu, X., Guo, J., Xian, K., and Zhou, X. (2018). Hierarchical travel demand estimation using multiple data sources: a forward backward propagation algorithmic framework on a layered computational graph. *Transportation Research Part C: Emerging Technologies*, 96, 321–346.
- Ying, L., Zhu, J., Huiyan, W., and Zhenyu, L. (2016). A novel method for estimation of dynamic OD flow. *Procedia Engineering*, (137), 94–102.
- Zhang, C., Osorio, C., and Flötteröd, G. (2017). Efficient calibration techniques for large-scale traffic simulators. *Transportation Research Part B: Methodological*, 97, 214–239.
- Zhou, X., Qin, X., and Mahmassani, H. (2003). Dynamic origin-destination demand estimation with multi-day link traffic counts for planning applications. *Transportation Research Record: Journal of the Transportation Research Board*, (1831), 30–38.